# PARAMETRIC RECONSTRUCTION FOR COMPLEX BUILDING FROM LIDAR AND VECTOR MAPS USING A DIVIDE-AND-CONQUER STRATEGY

T. A. Teo *

Center for Space and Remote Sensing Research, National Central University, Jhungli, Taoyuan 32001, Taiwan,China – teoteeann@gmail.com

**Commission III, WG III/3**

**KEY WORDS:** Laser scanning (LiDAR), Building reconstruction, Computer vision, Feature extraction, Urban planning.

**ABSTRACT:**

Three-dimensional building modelling is an important aspect of object reconstruction in computer vision. In this investigation airborne laser scanning data and 2-D building boundaries extracted from vectorized topographic maps are combined to reconstruct 3-D building models. To be able to reconstruct a variety of buildings, both planar and circular roof elements are included. The proposed scheme is a divide-and-conquer approach which is comprised of two major parts: (1) the extraction of the building primitives; and (2) the parametric shaping of the building roofs. The inner structural lines are extracted first. The complex buildings are then divided into several primitives based on the extracted lines. The roof for each building primitive is formed from the laser scanning point clouds. Finally the roofs and base heights of building are combined to obtain 3-D models. Two sample sites, with different building characteristics, are tested for the purposes of validation. The experimental results indicate that the proposed scheme allows for quite high fidelity.

## 1. INTRODUCTION

### 1.1 Motivation and Goals

The importance of cyber city modelling is increasing due to the need for accurate 3-D spatial information for urban planning, construction, and management. A cyber city is simply a replica of a real city reconstructed in cyber space that can be stored in an information system. Such models are an essential part of urban and environmental planning, hazard mitigation, telecommunications, flight simulation, transportation planning, and map revision. In addition, the timely information they help to provide is valuable for the city management decision makers. The aim of this research is to automate the manual production of building modelling for cyber city.

### 1.2 Related Works

Building model is one of the most important and attractive elements in a cyber city. These 3-D building models are mainly reconstructed from aerial images, laser scanning point clouds and vector maps (Hu *et al.*, 2003). The first step of building reconstruction from aerial images is to extract the image features. One may then use the extracted features to model the buildings through a hypothesis process. This means that the crucial issue for building reconstruction from image data is to extract the building features. Reconstruction strategies based on laser scanning are mainly concerned with the detection of roof planes. The planar features are extracted first then used to derive the line features. The building model is obtained by integrating the planar and linear features.

Vectorized topographical maps provide accurate two-dimensional building boundaries. In the traditional mapping process the building height is simplified in relation to the number of floors. The elevation of each floor has a certain value and from this unit of measurement (i.e., the number of floors) and the building boundaries we may generate rough 3-D prismatic building models. However, the accuracy and detail of these building models are insufficient for many applications. In order to improve the building details, the inclusion of different data in the building reconstruction process is needed (Schiewe, 2003).

Nowadays, other data sources, such as aerial images, laser scanning point clouds and vector maps, are generally available. Several data fusion algorithms have been proposed for the reconstruction of building models from these sources, e.g., laser scanning and aerial images (Rottensteiner, 2003), laser scanning and three-line-scanner images (Nakagawa *et al.*, 2002), laser scanning and high resolution satellite images (Guo, 2003), laser scanning and vector maps (Peternell and Steiner, 2003), vector maps and aerial image (Suveg and Vosselman, 2004). However the extraction of buildings from different sources is still one of the most challenging tasks. This however can be improved by fusing different sources, for example vector maps include accurate 2-D building boundaries while 3-D point clouds acquired by airborne laser scanning provide abundant shape information. The integration of these two complementary data sets makes it possible to reconstruct complex buildings. We propose here a scheme to reconstruct building models from the data fusion point of view, using laser scanning data and vector maps.

Several investigators have reported on the generation of building models from lidar and vector maps (Haala and Brenner, 1999; Vosselman and Dijkman, 2001). In the beginning, the 2-D ground plans are divided into rectangular primitives using a heuristic algorithm. For each of the 2-D primitives, a number of different 3-D parametric primitives from a fixed set of standard

* Corresponding author.

types are instantiated and their optimal parameters are estimated. The final building model is obtained by merging all 3-D primitives (Haala and Brenner, 1999). However, this method is restricted to the finite types of rectangular 3-D parametric primitives. Vosselman and Dijkman (2001) also use the concave ground plan corners to split the building into smaller primitives. In this study, additional structural lines from feature extraction are constrained to these primitives. Then, Hough-based planes extraction is selected to merge the segments. Finally, the building model is combined by the extracted roofs. The methods are suitable for planar roofs building reconstruction. But the curvilinear roofs are not considered in their investigations.

The general modelling procedure includes two major steps: the detection of the building regions and the reconstruction of the building models (Baillard and Maiter, 1999). Since ways to find the building boundaries are already available, in this research we focus on the reconstruction part. In this investigation we handle flat, gabled, cylindrical and spherical roofs, by the fusion of building boundaries and airborne laser scanning point clouds.

### 1.3 The Need for More Investigation

Reconstruction strategies can be classified into two categories, i.e., model-driven and data-driven. The model-driven strategy is a top-down strategy, which starts with a hypothetical building model which is verified by the consistency of the model with the laser scanning point clouds. The data-driven strategy is a bottom-up strategy where the planar and linear features are extracted in the beginning, then grouped into a building model through a hypothesizing process. These two strategies have their advantages and limitations. A hybrid strategy may overcome the limitation of each strategy. However, the generation of building models by hybrid method has seldom been discussed.

### 1.4 The Purposed Method

The proposed scheme is comprised of two major parts: (1) the extraction of the building primitives, and (2) the parametric shaping of the building roofs. Since the building boundaries provide important clues as to the interior roof structure, complex buildings are divided into several simple building primitives. The complex building is then reconstructed by combining all the building primitives. The initial structural lines are first extracted from the laser scanning data then refined based on the building boundaries through a geometric regularization process. Once the structural lines are extracted, the building boundaries are divided into several building primitives using the extracted lines. The surface function can be determined by fitting the point clouds. In the shaping process, the roof for each building primitive is determined from the laser scanning point clouds. The roof shapes include both planar and circular types. Finally, the roofs and base heights of the building are combined to obtain the building models.

## 2. METHODOLOGY

This method utilizes a divide-and-conquer strategy to perform the building modeling. First, the building is divided into several building primitives; the building models are then reconstructed from the building primitives. This hybrid method integrates the ideas of data-driven in primitive extraction and the ideas of model-driven in shape fitting. The scheme includes two major parts: (1) the extraction of the building primitives, and (2) the shaping of the building roofs. A flow chart of the building reconstruction is shown in Figure 1.

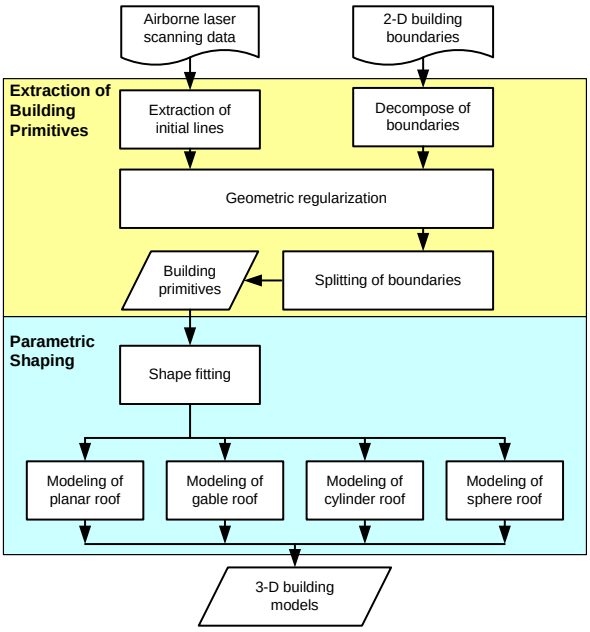


Figure 1. Flowchart of the proposed method

### 2.1 Extraction of Building Primitives

Most complex buildings can be described as an aggregation of simple building parts. The objective of primitive extraction is to divide the building polygon into several simple units. This is done by extracting the inner structural lines from the laser point clouds. These lines can include both step edges and ridge lines. A step edge (also called a height jump or wall) is a line between two different heights or structural facets. A ridge line indicates a structural line on a gable roof that may be viewed as the intersection of two facets. According to the design procedure, step edges are extracted from during this stage while ridge lines are determined after primitive extraction. There are four major steps in this part: (1) extraction of initial lines, (2) decomposition of building boundaries, (3) geometric regularization, and (4) splitting of building boundaries.

In the extraction of initial lines, the laser scanning data are first interpolated as grid data. Since the point elevations are represented as pixel values, we may use an image processing technique to treat the grid data. The edge features are obtained by using the Canny edge detector (Canny, 1986), which extracts the location of discontinuities or sharp changes in elevation. After extracting the edge features, straight line tracking using a strip algorithm (Leung and Yang, 1990) is performed. The algorithm extracts straight lines within a pipe line, that is, by including adjacent pixels for a given width. Once the straight lines are extracted, a length threshold is applied to remove any short lines caused by random noise. Figure 2a shows an example of the initial line extraction. The extracted lines do not meet the concave corners in this stage.

For the decomposition of building boundaries, the building boundaries are delineated by closed polygons. Building boundaries often provide useful clues about the location of structural lines (Suveg and Vosselman, 2004). In this study, we

decompose the building boundaries to form the building primitives. The decomposition is done by extending boundary lines. All extended lines inside the building are retained. Figure 2b demonstrates the results. The solid lines indicate building boundaries while the dotted lines indicate the extended lines.

During geometric regularization, the initial lines are regularized by employing geometric constraints. The end points of the initial lines are adjusted to the most probable locations based on the decomposed building lines. If the initial lines are in a pipeline, they are adjusted to coincide with the decomposed lines. Figure 2c illustrates the results of geometric regularization based on decomposed lines.

In the next step, the splitting of building boundaries, the building polygon is split into several building primitives, based on the structural lines. Each building primitive represents a small element of the building. The split and merge process comprises the two major steps to primitive generation. All structural lines are extended to the building boundaries, after which their intersection points are calculated. In other words the building polygon is first split into smaller polygons then merged based on examination of the lines shared between polygons. Figure 2d illustrates the generation of building primitives during building modelling. In this example, the building is split into three polygons.

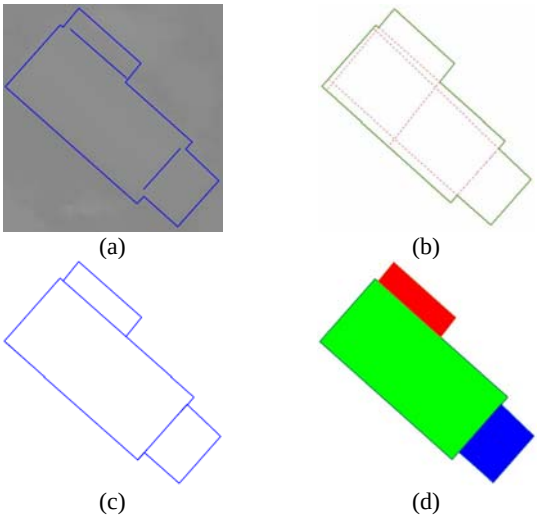


Figure 2. Illustration of the extraction of building primitives: (a) Initially extracted lines; (b) decomposition of building boundaries; (c) structural lines after geometrical regularization; (d) building primitives

### 2.2 Shaping of the Building Roofs

The objective of this step is to shape the roofs of each building primitive. Only the laser scanning point clouds from within the building primitives are used to perform the building shaping. The building primitive is shaped. A least squares fitting is used to minimize the point-to-surface distance (Rabbani and Heuvel. 2004). ***Flat roofs*** are the simplest. We use the plane equation shown as Equation 1 to assign the roof height.

For a ***gabled roof***, TIN-based region growing (Schroder and Robbach, 1994) is used to detect the facets and extract the ridge lines. The coplanarity and adjacency between triangles are considered in TIN-based region growing. The coplanarity condition means that the distance from the triangle's center to the plane is small. When the triangles meet the coplanarity criteria, they are merged together as a new facet. The process starts by selecting a seed triangle and determining the initial plane parameter. If the distance from a neighbouring triangle to the initial plane is smaller than the threshold, these two triangles are combined. The reference plane parameter is recalculated using all of the triangles that belong to the region. The seed region continues to grow as long as the distance does not exceed a specified threshold. A new seed triangle is chosen when the region stops growing. The region growing step stops when all triangles have been examined. However due to errors in the laser scanning data, fragmented triangles may exist in some detected regions. In this case small regions will be merged with the neighbourhood that has the closest normal vector. Once the planar segments are extracted, the ridge line is obtained by determining the intersection of two adjacent planar faces. A gabled roof is indicated by the ridge lines.

In order to reconstruct a ***cylindrical roof***, the circle equation, i.e. Equation 2, is utilized to obtain the curvilinear parameter. In the first step the specific directions indicated by the 3-D point clouds is determined, i.e. the main building direction, then, the circle equation is selected as the target equation for the parametric shape fitting. An example of re-projected laser scanning point is shown in figure 3. Considering the commonality of polyhedral models in building representation for a cyber city, each cylinder is reformed to be a polyhedron. The spherical equation, i.e. Equation 3, is used to model the ***spherical building roof***. The sphere is also transformed into a polyhedral model. After modelling the roofs, the terrain elevations are used to determine the building base height. Finally, the 3-D building model is obtained by merging all 3-D building primitives. Figure 4 demonstrates the results of building modelling for each roof types.

$$Z = a\,X + b\,Y + c, \tag{1}$$

$$R_2 = (U - U_0)^2 + (V - V_0)^2, \tag{2}$$

$$R_3 = (X - X_0)^2 + (Y - Y_0)^2 + (Z - Z_0)^2, \tag{3}$$

where:
X, Y, Z: the coordinates of the laser scanning point;
U, V: the coordinates of the projected laser scanning point;
a, b, c: the coefficients of the plane equation;
$R^2$, $U_0$, $V_0$: the coefficients of the circle equation;
$R^3$, $X_0$, $Y_0$, $Z_0$: the coefficients of the spherical equation.

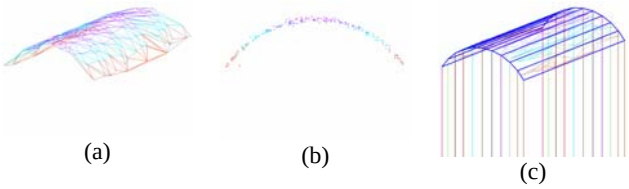


Figure 3. Illustration of point re-projection for cylindrical roof: (a) perspective view of laser scanning points; (b) re-projected laser scanning points; (c) cylindrical roof model

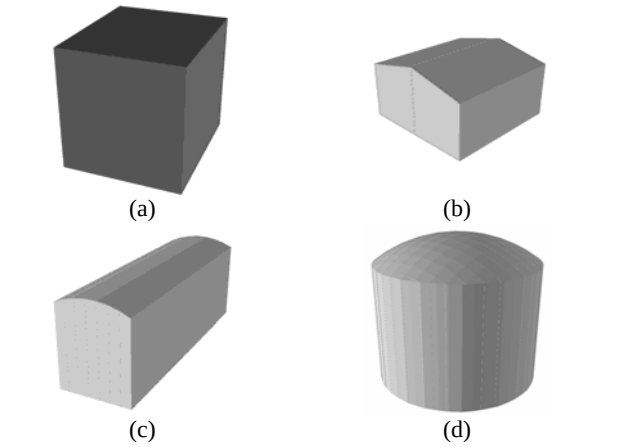

(a) (b) (c) (d)

Figure 4. Example of building models: (a) Flat; (b) gabled roof; (c) cylindrical roof; (d) spherical roof

## 3. EXPERIMENTAL RESULTS

Two test sites, including buildings with different characteristics, are selected for the validation process. The first one covers a sub-urban area located near Ping-Dong city in southern Taiwan. The second case covers an urban area located in Taipei city in northern Taiwan.

### 3.1 Case I

The laser scanning data used in this research covered an area of 200m by 170m. The data set was obtained by a Leica ALS 50 system. The accuracy of the acquired point cloud was better than 0.2m. The average point density was 2.0 pts/$m^2$. The discrete points were also rasterized to fit raster data with a pixel size of 0.5m. The vector maps used had a scale of 1:1,000 with an estimated accuracy of 0.5m. Figure 5a shows the laser scanning point clouds overlapped with the vector maps. Seventy-eight building polygons existed in the test area with the four roof types. Figure 5b shows the results of primitive extraction. After the extraction, the number of building polygons increased from 78 to 123. The increase in the number of polygons indicates that the amount of detail has been augmented. The total number of flat and gabled roofs in the test site was 102 and 18 respectively. There were two cylindrical roofs and one spherical roof in the test site.

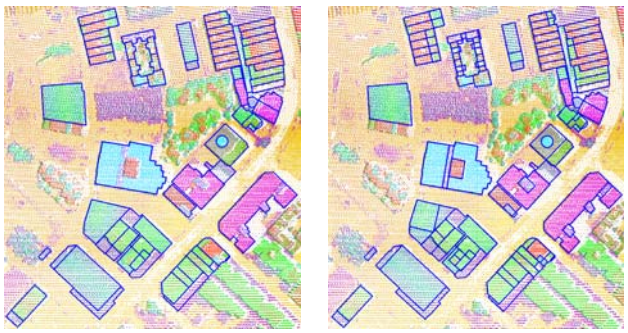

(a) (b)

Figure 5. Test data for Case I : (a) Point clouds with building boundaries; (b) results of primitive extraction

After the extraction of building primitives, different surfaces were tested to perform building shaping for each primitive. The generated digital building models (DBM) are shown in Figure 6.

After including the interior roof structure, the number of building polygons increased further from 123 to 189. A comparison of original building boundaries to the generated building models shows that the more detail is preserved in the models. An example with a complex building is shown in Figure 7.

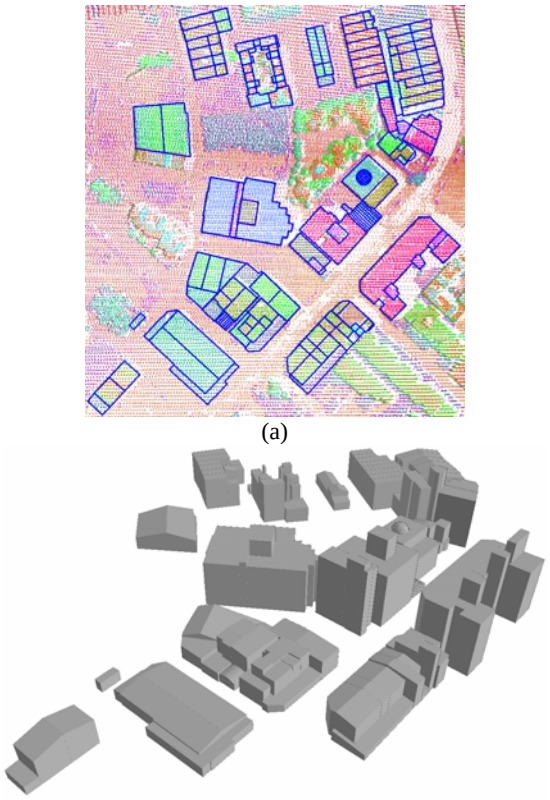

(a) (b)

Figure 6. Results of generated building models:(a) Top-view of the generated models; (b) perspective view of the generated models

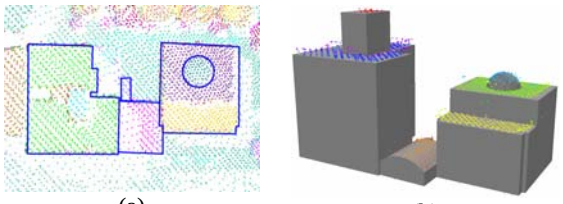

(a) (b)

Figure 7.An example of reconstruction for complex buildings: (a) Original boundaries with point clouds; (b) generated model with the original point clouds

### 3.2 Case II

The lidar data used in this case are located in Taipei, a metropolis in northen Taiwan. This area includes various types of buildings such as high-rise building and complex building. The data set was also obtained by a Leica ALS 50 system in Aug, 2007. The average density of the lidar point clouds was 10 pts/m2. The discrete lidar points were also rasterized to DSM with a pixel size of 0.3m for step edge extraction. The vector maps used have a scale of 1:1,000. Figure 8 shows the lidar points overlapping the vector maps. The test area is about 950m by 1210m in size. We select 39 building groups in the test area

with different roof types that include flat, slant, gable, and cambered roofs.

Figure 8. Point clouds with building boundaries of Case II

The top-view and perspective-view of reconstructed DBM is shown in Figure 9. After including the interior roof structure, the number of building polygons increased further from 158 to 557. A comparison of vector maps with the generated building models showed that the models preserve more detail than the vector maps. The flat roof was the simplest shape and with the largest number of 262. This area contains 7 slant, 30 gable, 9 camber and 2 sphere roofs. The result indicated that the non-flat roofs were split into many small polygons to represent the non-linear roof tops. For example, two sphere roofs were split into 149 small polygons.

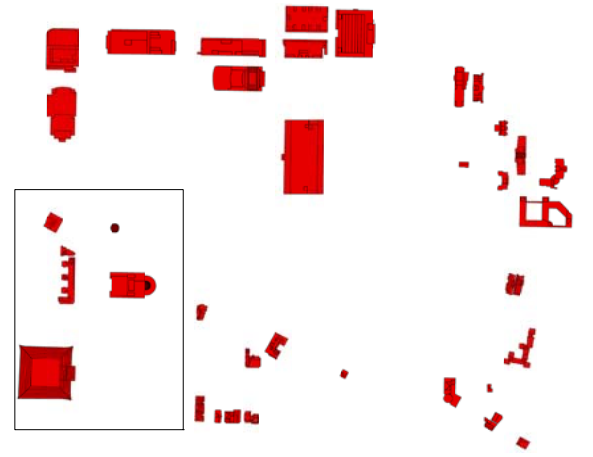

**(a)**

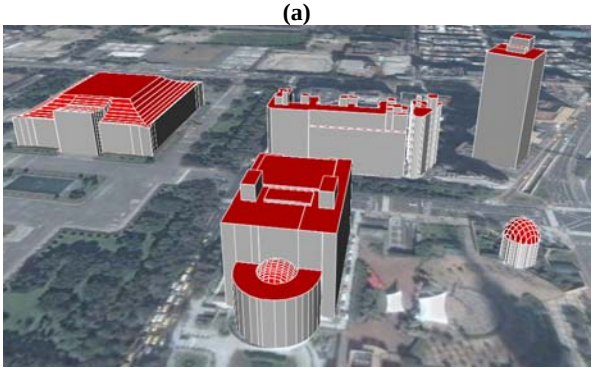

(b)

Figure 9. Results of generated building models:(a) Top-view of the generated models; (b) perspective view of the generated models

### 3.3 Validation

The experimental validation procedure includes three aspects. First the ***fidelity***, i.e., the reconstruction rate for different building types is validated. Second the ***height consistency*** between the reconstructed roof tops and the original lidar point clouds is checked. Third the ***planimetric accuracy*** between the reconstructed roof and the structural lines from stereo images is evaluated. The reference data is the digital aerial images with 17.5cm spatial resolutions. By comparing the reconstructed building and the stereo images, we provided the fidelity of reconstruction rate. Table 1 shows the fidelity test of these two cases. In Case I, the overall omission error was 12% while the point density is about 2pts/$m^2$. Most of the missing building polygons were the small polygons which were smaller than 10$m^2$. The completeness of reconstructed building was 87% for Case I. For Case II, the overall omission error was 4% while the completeness of reconstructed building reached 92% in this urban area. Overall, 92% of buildings had been reconstructed correctly.

| Case | Omission Polygon | Reconstructed Polygon | Correct Polygon | True | Omission Error | Completeness |
|---|---|---|---|---|---|---|
| | ( O ) | ( T ) | ( S ) | ( GT ) | ( O/GT ) | ( S/GT ) |
| I | 26 | 189 | 188 | 205 | 12.09% | 87.44% |
| II | 24 | 557 | 540 | 586 | 4.10% | 92.15% |
| All | 50 | 746 | 728 | 791 | 6.32% | 92.04% |

Table 1. Fidelity check

Since shaping performance is our major concern, the original point clouds are used to evaluate the relative accuracy. The distance from point-to-roof is examined to validate the shaping error. The roof-top planes in the reconstructed models are compared to the original point clouds; the root-mean-square-errors (RMSE) were 0.54m and 0.55m for Case I and II, respectively. Moreover, the mean of the shaping error was smaller than 0.1m for both cases. Figure 10 shows the histogram of the shaping error.

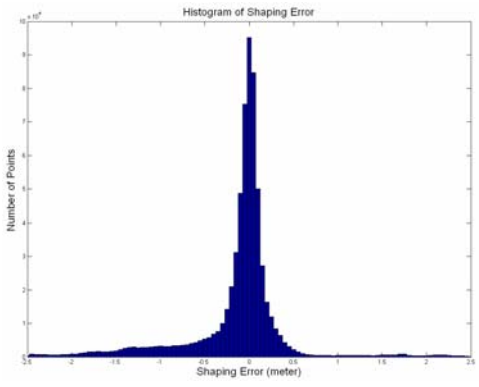


Figure 10. Histogram of shaping errors

For planimetric validation, we compared the coordinates of the roof corners in the reconstructed models with the ones acquired by stereoscopic manual measurements. We measured 252 well-defined building corners for accuracy evaluation. The building corner is the intersection of extracted structural lines. In other words, the target for examination is not the building boundaries from the topographic map. The RMSE of these corner points

were 0.40m and 0.41m in the E and N directions, respectively. Figure 11 represents the distribution of errors. The x-axis shows the error in E direction while the y-axis is the error in N direction. The results revealed that the errors are not in systematic distribution. Most of the errors larger than 1m were located in the step-edge which was shorter than 3m. Hence, the extraction of short step-edge from lidar points was not as accurate as ridge line.

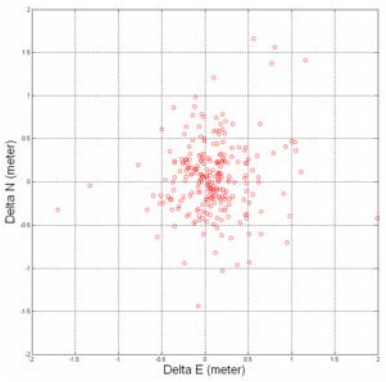


Figure 11. Planimetric errors of generated building corners

### 3.4 Discussion

This investigation has proposed a divide-and-conquer scheme to reconstruct a variety of buildings that integrates vector maps and lidar point clouds. The exiting inner structure lines from vector maps are beneficial to the building shaping. Normally, these inner lines are not exiting in the vector maps, but some of them are exception. For the complex buildings, these inner lines are still not enough to represent the building details. Comparing the original building lines and generated structure lines, the number of structure lines increased in both cases. The point density is an important factor in building extraction. The experiment indicates that the higher point density may improve the omission error especially the small building polygon.

## 4. CONCLUSIONS

In this research, a scheme for the reconstruction of building models via the merging of laser scanning data and building boundaries is investigated. The results from the tests demonstrate that our method has good potential for reconstructing buildings with planar, gabled, cylindrical and spherical roof types. The building models generated by the proposed method combine high horizontal accuracy from the building boundaries, and high vertical accuracy from the laser scanning data. In the validation, the reconstruction rate was better than 90% while the omission error was smaller than 7%. The planimetric accuracy of the reconstructed models was better than 0.5m while shaping error of the height of the reconstructed roofs was 0.55 m. Note that the small shaping bias, i.e. -0.10m, can be ignored.

## ACKNOWLEDGEMENTS

The author would like to thank Prof. Liang-Chien Chen of National Central University for his advice in this research. This investigation was partially supported by the National Science Council of Taiwan under Project No. NSC 95-2221-E-008-103 and the Ministry of The Interior of Taiwan under Project No. H950925.

## REFERENCES

Baillard, C., Maiter, H. 1999. 3-D Reconstruction of Urban Scenes from Aerial Stereo Imagery: A Focusing Strategy, *Computer Vision and Image Understanding*, Vol. 76, No. 3, pp. 244-258.

Canny, J. 1986. A Computational Approach to Edge Detection. *IEEE Transactions on Pattern Analysis and Machine Intelligence*. Vol. 8, pp.679-698.

Guo, T. 2003. 3D City Modeling using High-Resolution Satellite Image and Airborne Laser Scanning Data. Doctoral dissertation, Department of Civil Engineering, University of Tokyo, Tokyo.

Haala, N., and C. Brenner, 1999. Virtual city models from laser altimeter and 2D map data, Photogrammetric Engineering & Remote Sensing, Vol. 65, No. 3, pp. 787-795.

Hu, J., You, S., Neumann, U. 2003. Approaches to Large-Scale Urban Modeling. *IEEE Computer Graphic and Applications*, Vol. 23, No. 6, pp. 62-69.

Leung, M.K., Yang, Y.H. 1990. Dynamic Strip Algorithm in Curve Fitting, *Computer Vision, Graphics and Image Process*, Vol. 51, pp. 146-165.

Nakagawa, M., Shibasaki, R., Kagawa, Y. 2002. Fusion Stereo Linear CCD Image and Laser Range Data for Building 3D Urban Model. *International Achieves of Photogrammetry and Remote Sensing*. Vol. 34, pp. 200-211.

Peternell, M., Steiner, T. 2003. Reconstruction of Piecewise Planar Objects from Point Clouds, *Computer-Aided Design*, Vol. 36, pp. 333-342.

Rabbani, T., Heuvel, F.A. van den. 2004. Methods For Fitting CSG Models to Point Clouds and Their Comparison. *Proceeding of The 7th IASTED International Conference on Computer Graphics and Imaging*, pp. 279-284.

Rottensteiner, F. 2003. Automatic Generation of High-Quality Building Models from Lidar Data, *IEEE Computer Graphic and Applications*, Vol. 23, No. 6, pp. 42-50.

Schiewe, J. 2003. Integration of Data from Multi-sensor Systems for Landscape Modeling Tasks, *Proceeding of Joint ISPRS Workshop "Challenges in Geospatial Analysis, Integration and Visualization II"*, unpaginated CD-Rom.

Schroder, F., Robbach, P. 1994. Managing the Complexity of Digital Terrain Models. *Computer and Graphics*, Vol. 18, pp. 775-783.

Suveg, I. Vosselman, G. 2004. Reconstruction of 3D Building Models from Aerial Images and Maps, *ISPRS Journal of Photogrammetry & Remote Sensing*, Vol. 58, pp. 202-224.

Vosselman, G., Dijkman, S., 2001. 3D building model reconstruction from point clouds and ground plans. *International Achieves of Photogrammetry and Remote Sensing*. Vol. 34, Part 3/W4, pp. 37-43.